ISSN 1070-3632, Russian Journal of General Chemistry, 2015, Vol. 85, No. 5, pp. 1125–1131. © Pleiades Publishing, Ltd., 2015.
Original Russian Text © A.V. Pulya, I.I. Seifullina, L.S. Skorokhod, V.G. Vlasenko, Ya.V. Zubavichus, S.I. Levchenkov, 2015, published in Zhurnal Obshchei Khimii, 2015, Vol. 85, No. 5, pp. 831–837.

Self-Assembly in the MnX_2–2-(7-Bromo-2-oxo-5-phenyl-2,3-dihydro-1*H*-1,4-benzodiazepin-1-yl)acetohydrazide–Salicylic Aldehyde Systems: Composition, Structure, and Properties of the Products

A. V. Pulya[a], I. I. Seifullina[a], L. S. Skorokhod[a], V. G. Vlasenko[b], Ya. V. Zubavichus[c], and S. I. Levchenkov[d]

[a] *Mechnikov Odessa National University, ul. Dvoryanskaya 2, Odessa, 65082 Ukraine e-mail: lborn@ukr.net*
[b] *Scientific Research Institute of Physics, Southern Federal University, Rostov-on-Don, Russia*
[c] *Russian Scientific Center "Kurchatov Institute," Moscow, Russia*
[d] *Southern Scientific Center, Russian Academy of Sciences, Rostov-on-Don, Russia*

Received January 15, 2015

Abstract—Complexes of Mn(II) with 2-(7-bromo-2-oxo-5-phenyl-2,3-dihydro-1*H*-1,4-benzodiazepin-1-yl)-acetohydrazide and product of its condensation with salicylic aldehyde have been prepared and characterized by elemental analysis, IR spectroscopy, electrical conductivity, and magnetic susceptibility. Thermal stability of the complexes has been characterized. Structure of the coordination node of the complexes has been determined by X-ray absorption spectroscopy.

Keywords: coordination compound, manganese(II), 2-(7-bromo-2-oxo-5-phenyl-3*H*-1,4-benzodiazepin-1-yl)-acetohydrazide, salicylic aldehyde

DOI: 10.1134/S1070363215050205

Study of the features of the interaction of organic drugs with metal ions and development of more efficient pharmaceutically active compounds is among the major tasks of modern bioinorganic chemistry.

We have earlier used 2-(7-bromo-2-oxo-5-phenyl-2,3-dihydro-1*H*-1,4-benzodiazepin-1-yl)acetohydrazide (Hydr) known as Hydazepam [1] as a ligand to prepare the corresponding coordination complexes of Co^{2+} and Ni^{2+} [2, 3]. We have also studied the interaction of $MnCl_2$ with Hydr and the product of condensation of the latter with pyrotartaric acid (HPv). Structures of the prepared coordination compounds $[Mn(Hydr)_2Cl_2]$ and $[Mn(HydrHPv)_2Cl_2]$ have been confirmed by ESR and IR spectroscopy as well as electrical conductivity and magnetic susceptibility measurements [4].

Extending these studies, herein we report on preparation of coordination compounds via self-assembly in the MnX_2–Hydr–HSal systems (X = Cl^-, CH_3COO^-, or salicylic aldehyde HSal; ethanol–isopropanol mixture was used as solvent).

The $[Mn(HydrSal)_2]$ (**I**) and $[Mn(HydrSal)\cdot CH_3COO(C_2H_5OH)_2]$ (**II**) complexes (Table 1) were isolated from the MnX_2–Hydr–HSal–C_2H_5OH systems, with the ligand being the product Hydr condensation with salicylic aldehyde.

Complexes **I** and **II** were fine-crystalline compounds insoluble in methanol, ethanol, isopropanol, chloroform, and acetonitrile but soluble in DMSO and DMF. Their effective magnetic moments (Table 1) corresponded to octahedral coordination of Mn(II) [5].

According to the electrical conductivity of 1×10^{-3} M. of the solutions in DMSO (Table 1), complexes **I** and **II** were non-electrolytes [6].

TGA studies of the complexes **I**, **II**, and $[Mn(Hydr)_2Cl_2]$ (**III**) (Table 2) revealed that their thermal decomposition was a stepwise process. Compound **III** was stable up to 290°C, its decomposition being accompanied with endothermic effect of dehydrochlorination, followed by two exothermic effects assigned to the oxidative thermal decomposition. Thermolysis of com-

Table 1. Elemental analysis data, molar conductivity, and magnetic susceptibility of complexes **I** and **II**

Comp. no.	Found, %					Formula	Calculated, %					Molar conductivity, Ω^{-1} cm^2 mol^{-1}	μ_{eff}, μ_B (292 K)
	C	H	N	Br	Mn		C	H	N	Br	Mn		
I	55.58	3.31	10.75	15.27	5.16	$[Mn(C_{24}H_{20}BrN_4O_3)_2]$	55.65	3.48	10.82	15.46	5.31	16.3	5.94
II	55.67	4.68	8.11	11.30	7.82	$[Mn(C_{30}H_{33}BrN_4O_7)]$	51.72	4.74	8.05	11.49	7.90	10.3	6.00

Table 2. Thermal gravimetry analysis of complexes **I**–**III**

Comp. no.	Temperature range ΔT (t_{max}, °C)↑↓	Δm (TG), %	Δm_{theor}, %	Thermal decomposition product (MnO)	
				m_{theor}, %	m_{exp}, %
I	290–390 (340)↑	12.5	Oxidative thermal decomposition	6.85	6.50
	390–730 (620)↑	37.5			
	730–920 (800)↑	72.5			
II	100–230 (130)↓	6.8	6.61 (–C_2H_5OH), oxidative thermal decomposition	10.17	10.00
	230–360 (340)↑	15.2			
	360–460 (380)↑	20.0			
	460–690 (620)↑	49.0			
III	290–310 (300)↓	7.5	7.89 (–2HCl), oxidative thermal decomposition	7.89	8.01
	310–650 (570)↑	22.0			
	650–920 (900)↑	40.0			

plex **I** occurred as three overlapping exothermic effects of oxidation of the organic part of the molecule and deep decomposition. A special feature of thermal decomposition of complex **II** was the observed low-temperature endothermic effect assigned to elimination of one ethanol molecule. The following three stages were accompanied with exothermic effects and the steady mass loss. The high-temperature thermolysis product of the studied complexes was MnO.

Coordination type of the ligands was elucidated by means of IR spectroscopy by comparing the characteristic vibration frequencies of the free ligands and the corresponding bands in the spectra of complexes **I**–**III**. In particular, the spectra of complexes **I** and **II** contained no bands assigned to the amino group; however, a new band due to the ν(C=N) vibration appeared at 1621 (**I**) or 1613 (**II**) cm^{-1}. The ν(C=N) band position pointed out that the ligand present in the complexes was a product of condensation of the hydrazide amino group and the carbonyl group of salicylic aldehyde; hence, the ligand was a hydrazone. The hydrazide stretching band was shifted towards lower frequencies in the course of the complex formation [1678 (Hydr), 1666 (**I**), and 1644 (**II**) cm^{-1}], evidencing about coordination of that group with Mn^{2+}. Similar shift was observed in the case of the salicylic aldehyde phenol ν(C–O) band: 1200 (HSal), 1154 (**I**), and 1156 (**II**) cm^{-1}, typical of the OH group coordinated in the deprotonated form.

IR spectrum of complex **II** contained the absorption band of acetate ion ν(CO_2^-) at 1645 cm^{-1} [7]. Noteworthily, the spectra of complexes **I** and **II** contained new bands at 514 and 446 cm^{-1} (**I**) and 510 and 450 cm^{-1} (**II**), assigned to the ν(Mn–O) and ν(Mn–N) vibrations, respectively.

Effective magnetic moments of the complexes of 5.94 μ_B (**I**) and 6.00 μB (**II**) at 292 K (Table 1) were practically independent of temperature, being close to the purely spin μ_{eff} value and typical of the mononuclear octahedral Mn(II) complexes.

Structure of the coordination node in complexes **I**–**III** was studied by means of XANES spectroscopy. The normalized XANES curves of Mn*K* absorption

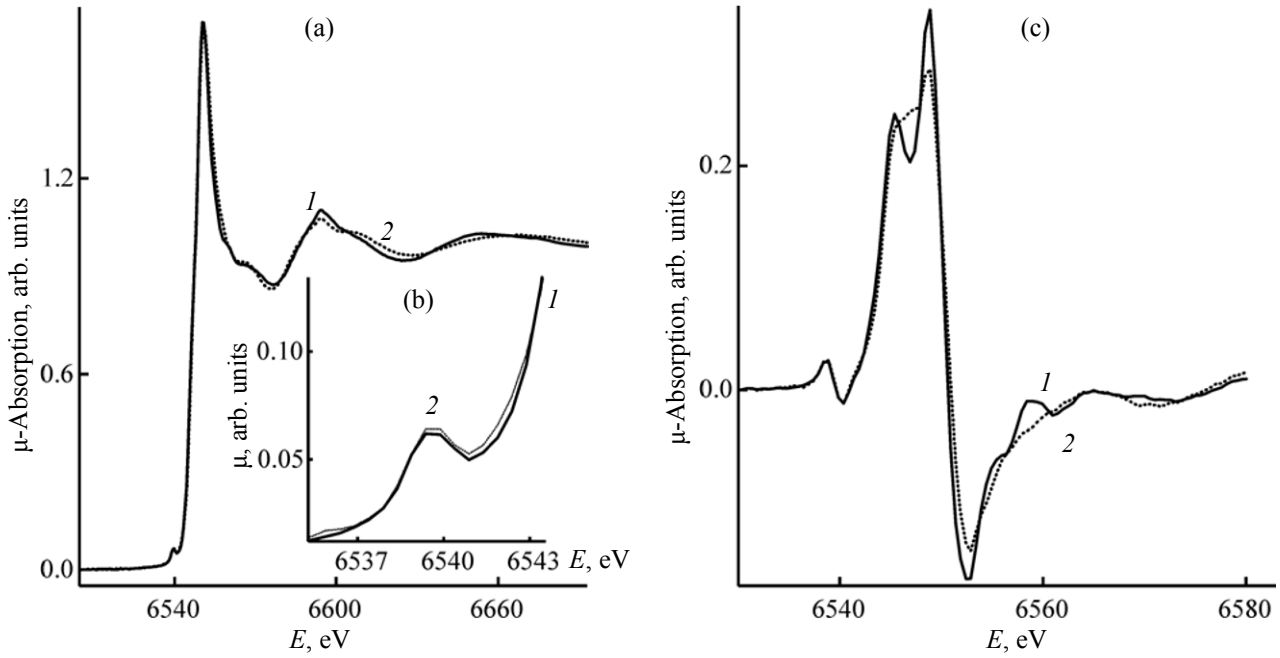

Fig. 1. Normalized XANES spectra of Mn*K* edges of absorption (a) for complexes **III** (*1*) and **I** (*2*), pre-edge region (b), and the corresponding first derivatives of the edges (c).

edges and their first derivatives are shown in Figs. 1 and 2; the inserts display the enlarged representation of the pre-edge structure of the X-ray absorption spectra. As seen from Fig. 1, the shape and parameters of XANES spectra of compounds **I** and **III** were close; however, the first derivatives of the XANES curves were different in the degree of splitting of the major maximum. The pre-edge XANES curves of the both samples were strong; the peaks maximums and the integral intensities were practically identical. The origin of the pre-edge structure was due to the $1s \rightarrow 3d$ electronic transitions, dipole-forbidden for the *K*-edges of 3*d* metals. However, the 4*p*–3*d* hybridization of the metal atomic orbitals occurred in the absence of the inversion center of the coordination node, and the intensity of the pre-edge structure was sharply increased (the hybridization is strictly forbidden for the centrally symmetrical coordination polyhedrons, in particular, for octahedron; in such cases the pre-edge peak intensity is predominantly determined by the $1s \rightarrow 3d$ quadrupole transitions, their contribution being two orders of magnitude lower than that of the dipole transitions). Hence, the manganese atom surrounding in the complexes **I** and **III** was low-symmetrical.

XANES spectra of complex **II** (Fig. 2) contained a large-amplitude pre-edge peak A, and the first derivative of the edge was split, pointing at the more distorted surrounding of manganese ion in that compound.

Quantitative parameters of local atomic surrounding of Mn^{2+} ion in the complexes **I**–**III** were determined from analysis of EXAFS of Mn*K* edges of the X-ray absorption spectra. Fourier transform magnitudes (FTM) of the EXAFS Mn*K* edges of the complexes **I**–**III** are shown in Fig. 3. It is to be seen that FTM of the complexes **I** and **III** EXAFS consisted of the basic peaks at different distances *r* [1.76 Å (the amplitude of 5.5 a. u.) (**I**) and 1.88 Å (6.7 a. u.) (**III**)], unambiguously corresponding to the scattering at the nearest coordination spheres. The weak peaks at $r >$ 2.0 Å were assigned to the farther coordination spheres. In the case of the complex **II**, the FTM consisted of the major peak at $r = 1.67$ Å (6.3 a. u.).

Taking into account the suggested structures of complexes **I**–**III** and the possible ligands coordination, we selected a set of models of manganese complexes from the Cambridge Structural database, used for simulation of theoretical EXAFS Mn*K* edges.

The results of simulation of the local atomic surrounding parameters of complexes **I**–**III** with the appropriate choice of the structural models are collected in Table 3.

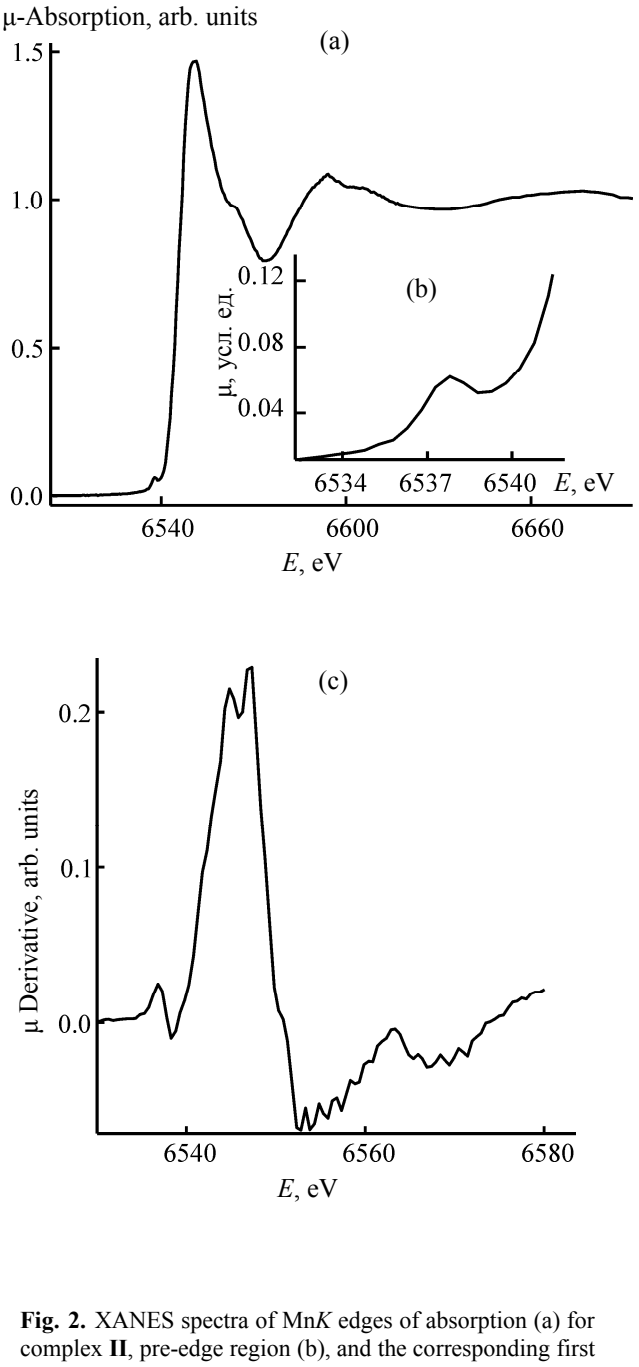

Fig. 2. XANES spectra of Mn*K* edges of absorption (a) for complex **II**, pre-edge region (b), and the corresponding first derivatives of the edges (c).

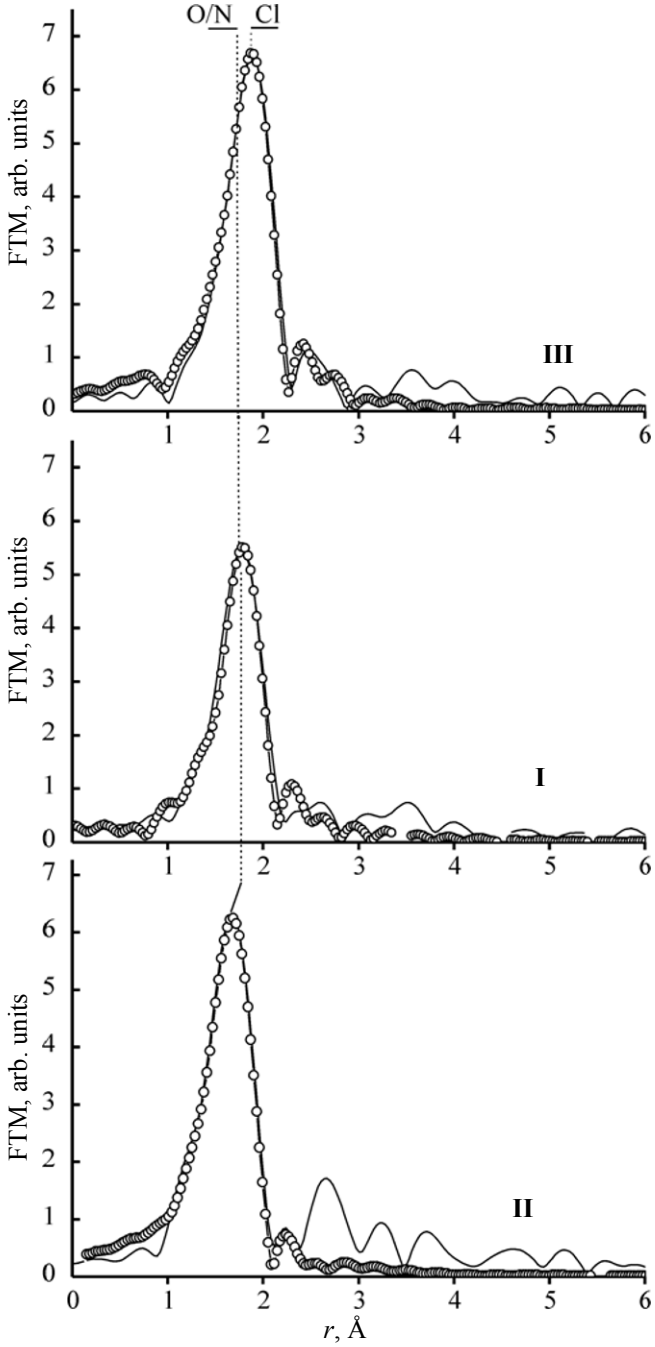

Fig. 3. Fourier transform magnitudes of the EXAFS Mn*K* absorption edges of complexes **I**–**III**.

In the case of complex **III**, the best model (leading to the lowest Q value) corresponded to the two axial chlorine atoms with the average Mn···Cl distance of 2.46 Å and the four Mn···O/N distances of 2.28 Å (Table 3). The similar distances were typical of a large set of model complexes from the Cambridge Structural Database.

The best model of complex **I** was a strongly distorted tetrahedron with the average Mn···O/N distances of 2.23 and 2.28 Å. The distances dispersion could be much larger in practice, as evidenced by a high Debye–Waller factor for those coordination spheres.

Several models were built for complex **II**, including hexa- as well as pentacoordinated Mn^{2+} nodes. The set of magnetochemical and X-ray absorption spectroscopy data pointed at the distorted octahedral surrounding of the coordination node as the best model, the parameters of the nearest coordination spheres being as shown in Table 3.

In summary, the following structures of complexes **I–III** were suggested basing on the results obtained via the independent physico-chemical methods (Scheme 1).

EXPERIMENTAL

Thermogravimetric analysis was performed using a Q-derivatograph of the Paulik–Paulik–Erdey system. The specimens were heated in air from 20 to 1000°C at the rate of 10 deg/min (the specimen mass of 60–80 mg, open platinum crucible as the specimen holder, and calcined alumina as reference).

Table 3. Structural parameters of the nearest surrounding of manganese atoms in compounds **I–III** from EXAFS data fitting[a]

Comp. no.	*N*	*R*, Å	σ^2, Å^2	Atom	*Q*, %
I	4	2.23	0.0050	O/N	2.2
	2	2.28	0.0050	O/N	
II	3	2.10	0.0035	O/N	0.6
	1	2.22	0.0035	O/N	
	2	2.25	0.0035	O/N	
III	4	2.28	0.0050	O/N	0.5
	2	2.46	0.0060	Cl	

[a] *R*, interatomic distance; *N*, coordination number; σ^2, the Debye–Waller factor; *Q*, goodness of fit.

Molar conductivity of the 1×10^{-3} mol/L solutions of complexes **I–III** in DMSO was measured using an Ekonomiks-ekspert digital instrument, the electrolyte type was determined according to the reference tables

Scheme 1.

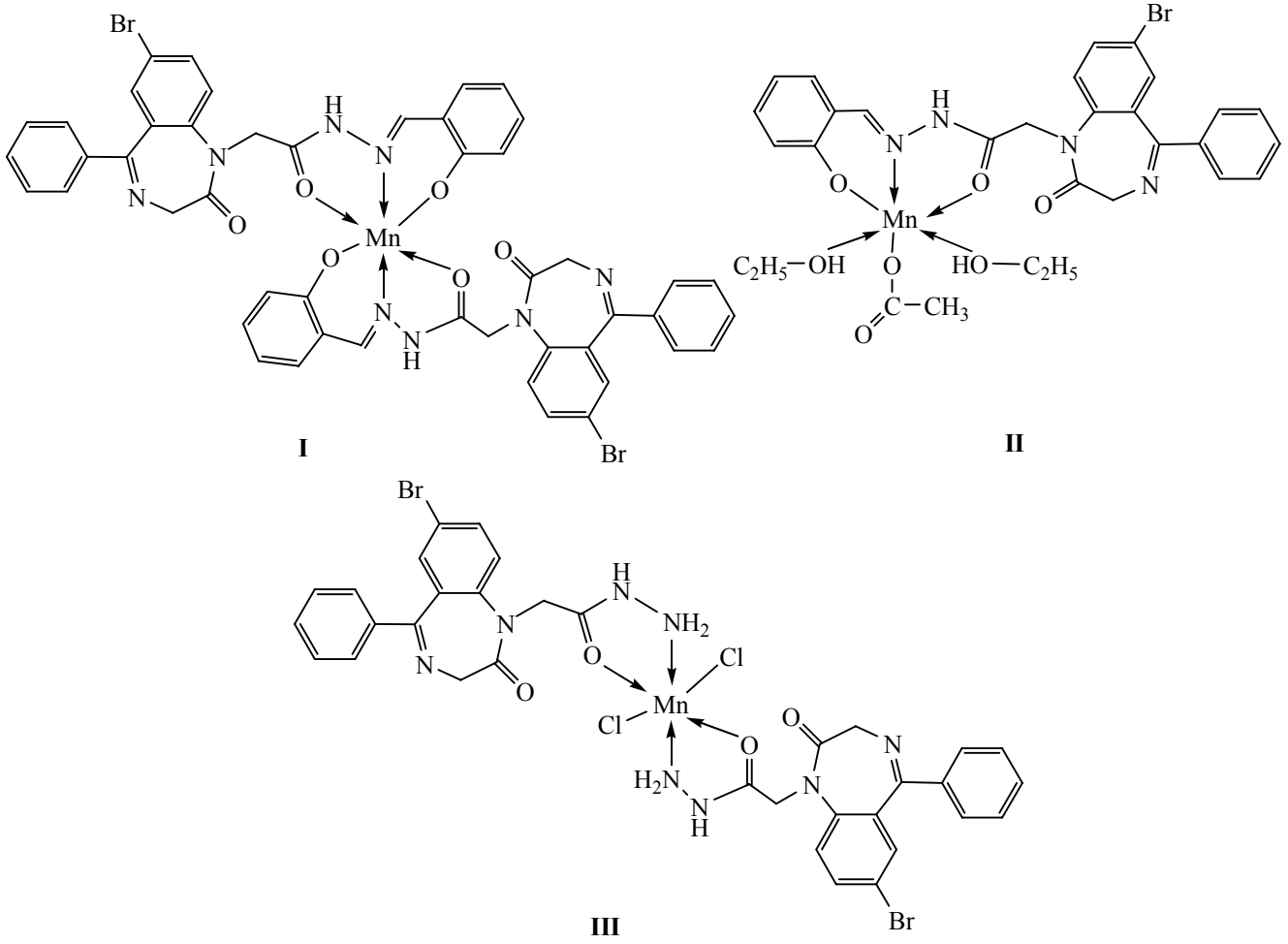

[6]. IR spectra of KBr pellets were recorded using Perkin–Elmer Spectrum BX-II FI-IR and Shimadzu FTIR-8400S spectrophotometers.

Specific magnetic susceptibility of the complexes was determined via a relative Faraday method at 77.4–292 K; $Hg[Co(CNS)_4]$ was used as calibration reference. The molar magnetic susceptibility ($\chi_м$) was calculated accounting for the atoms diamagnetism taking advantage of the additive Pascal scheme [8]. Effective magnetic moment was calculated as $\mu_{eff} = \sqrt{(3k/N\mu_B)\chi T} \approx \sqrt{8\chi T}$ with k the Boltzmann's constant; N, the Avogadro's number; and μ_B, Bohr's magneton.

X-ray MnK edges of the complexes **I–III** absorption were obtained in the transmission mode using the EXAFS spectrometer of the Structural Materials Science station of Kurchatov Synchrotron Center, Moscow. The X-ray beam monochromation was performed with a two-crystal Si(111) monochromator. The solid complex specimens were put between thin lavsan films.

The obtained spectra were processed taking advantage of the standard routines of background subtraction, normalization with respect to the K-edge jump, and extraction of the atomic absorption μ_0 [9]; the so prepared EXAFS (χ)-spectra were subject to Fourier transform at the wave vector of photoelectrons k ranging from 3.0 to 13.0 Å^{-1} with the k^3 weighing function. The derived FTM values represented the pseudo radial distribution of atoms in the nearest coordination spheres around the absorbing manganese atom, the coordination spheres radii being determined accurate within the phase corrections. The threshold ionization energy E_0 was selected according to the maximum of the first derivative of K edge and was then varied during fitting.

In order to extract the parameters of the nearest atomic surrounding of manganese ions, the experimental EXAFS spectrum was fitted with the $\chi^{(k)}$ function:

$$\chi(k) = S_0^2 \sum_{i=1}^{n} (N_i/R_i^2)[F_i(k)/k] e^{-2R/\lambda} e^{-2\sigma k} \sin(2kR_i + \Psi), \quad (1)$$

with N_i, number of atoms in the ith coordination sphere; R_i, average coordination sphere radius; σ_i^2, the Debye–Waller factor; $F_i(k)$, back scattering amplitude; k, wavenumber of the emitted electron.

Exact structural parameters of the nearest surrounding of manganese atoms in complexes **I–III** were determined via nonlinear fitting of the coordination spheres parameters aided by comparing the simulated EXAFS signal and that having been extracted from the full EXAFS spectrum by Fourier filtration of FTMs. The nonlinear fit was performed using IFFEFIT-1.2.11 software package [10]. The phases and amplitudes of scattering of the photoelectron wave required to simulate the model spectrum were computed using FEFF7 [11] software utilizing atomic coordinates of the structurally similar compounds.

The number of the multi-sphere fitting parameters never exceeded the number of independent parameters N_{ind} that could be in turn reliably determined from the given EXAFS spectrum in the Δk and Δr ranges:

$$N_{ind} = (2\Delta r \Delta k/\pi) + 1, \quad (2)$$

with Δk, analyzed range of the EXAFS spectrum in the space of photoelectron wave vector; Δr, the region of R-space over which the Fourier filtration was performed.

The goodness of fit function Q (the minimized fitting target parameter) was calculated as follows.

$$Q(\%) = [\Sigma(k\chi_{exp}k - k\chi_{th}k)^2/\Sigma(k\chi_{exp}k)^2] \times 100\%. \quad (3)$$

Elemental analysis of compounds **I** and **II** was performed as follows: content of carbon, hydrogen, and nitrogen was determined using a C,H,N-analyzer, bromine was determined by mercurimetry [12], manganese was determined by atomic emission spectro-scopy with inductively coupled plasma using an Optima–2100 DV device (Perkin–Elmer).

Complex **III** was prepared as described elsewhere [4].

Complexes I and II. 0.002 mol of salicylic aldehyde and ethanolic solution of $MnCl_2$ or $MnAc_2$ crystal hydrates (0.001 mol in 10 mL) were added to a solution of 0.002 mol of 2-(7-bromo-2-oxo-5-phenyl-2,3-dihydro-1*H*-1,4-benzodiazepin-1-yl)acetohydrazide in 20 mL of isopropanol. The reaction mixture was boiled on a water bath during 0.5 h. The precipitate formed after cooling the mixture was separated off, washed with isopropanol, with ethanol, and dried at 80°C to constant mass.

REFERENCES

1. *Gidazepam* (Hidazepam), Andronati, S.A., Kiev: Naukova Dumka, 1992.
2. Pulya, A.V., Seifullina, I.I., Skorokhod, L.S., Vlasenko, V.G., Zubavichus, Ya.V., Levchenkov, S.I., and

Pavlovskii, V.I., Abstracts of Papers, *X Mezhdunar. konf. "Spektroskopiya koordinatsionnykh soedinenii"* (X Int. Conf. "Spectroscopy of Coordination Compounds"), Tuapse, 2013, p. 225.

3. Pulya, A.V., Seifullina, I.I., Skorokhod, L.S., Vlasenko, V.G., Zubavichus, Ya.V., Levchenkov, S.I., and Pavlovskii, V.I., Abstracts of Papers*, XIX Ukrainskaya konf. po neorgan. khimii s mezhdunarodnym uchastiem* (XIX Ukrainian Conf. on Irganic Chemistry with International Participation), Odessa, 2014, p. 61.
4. Pulya, A.V., Seifullina, I.I., Skorokhod, L.S., Efimov, N.N., Ugolkova, E.A., and Minin, V.V., *Russ. J. Inorg. Chem*., 2015, vol. 60, no. 1, p. 51. DOI: 10.1134/S0036023615010106.
5. Neiding, A.B., *Magnetokhimiya kompleksnykh soedinenii perekhodnykh metallov* (Magnetochemistry of Complex Compounds of Transition Metals), Moscow: Nauka, 1970.
6. Geary, W.J., *Coord. Chem. Rev*., 1971, vol. 7, p. 81. DOI: 10.1016/S0010-8545(00)80009-0.
7. Nakamoto, K., *Infrared and Raman Spectra of Inorganic and Coordination Compounds*, Wiley, 1982.
8. Rakitin, Yu.V. and Kalinnikov, V.T., *Sovremennaya magnetokhimiya* (Modern Magnetochemistry), St. Petersburg: Nauka, 1994.
9. Kochubei, D.I., Baranov, Yu.A., Zamaraev, K.I., Vedrinskii, R.V., Kraizman, V.L., Kulipanov, G.N., Mazalov, L.N., Skrinskii, A.N. Fedorov, V.I., Khel'-mer, B.Yu., and Shuvaev, A.T., *Rentgenospektral'nyi metod izucheniya struktury amorfnykh tel: EXAFS-spektroskopiya* (X-Ray Method for Studying the Structure of Amorphous Solids: EXAFS-Spectroscopy), Novosibirsk: Nauka, Sib. Otd., 1988.
10. Newville, M., *J. Synchrotron Rad*., 2001,vol. 8, p. 96. DOI: 10.1107/S0909049500016290.
11. Zabinski, S.I., Rehr, J.J., Ankudinov, A., and Alber, R.C., *Phys. Rev*., 1995, vol. 52, p. 2995. DOI: 10.1103/PhysRevB.52.2995.
12. Klyuchnikov, N.G., *Rukovodstvo po neorganicheskomu sintezu* (Guide to Inorganic Synthesis), Moscow: Khimiya, 1965, p. 104.